nature materials

ARTICLES

PUBLISHED ONLINE: 4 DECEMBER 2017 | DOI: 10.1038/NMAT5039

# Topological order and thermal equilibrium in polariton condensates

Davide Caputo[1,2], Dario Ballarini[1]*, Galbadrakh Dagvadorj[3,4], Carlos Sánchez Muñoz[5], Milena De Giorgi[1], Lorenzo Dominici[1], Kenneth West[6], Loren N. Pfeiffer[6], Giuseppe Gigli[1,2], Fabrice P. Laussy[7,8], Marzena H. Szymańska[3] and Daniele Sanvitto[1,9]

**The Berezinskii–Kosterlitz–Thouless phase transition from a disordered to a quasi-ordered state, mediated by the proliferation of topological defects in two dimensions, governs seemingly remote physical systems ranging from liquid helium, ultracold atoms and superconducting thin films to ensembles of spins. Here we observe such a transition in a short-lived gas of exciton-polaritons, bosonic light–matter particles in semiconductor microcavities. The observed quasi-ordered phase, characteristic for an equilibrium two-dimensional bosonic gas, with a decay of coherence in both spatial and temporal domains with the same algebraic exponent, is reproduced with numerical solutions of stochastic dynamics, proving that the mechanism of pairing of the topological defects (vortices) is responsible for the transition to the algebraic order. This is made possible thanks to long polariton lifetimes in high-quality samples and in a reservoir-free region. Our results show that the joint measurement of coherence both in space and time is required to characterize driven–dissipative phase transitions and enable the investigation of topological ordering in open systems.**

Collective phenomena which involve the emergence of an ordered phase in many-body systems have a tremendous relevance in almost all fields of knowledge, spanning from physics to biology and social dynamics[1,2]. Although the physical mechanisms can be very different depending on the system considered, statistical mechanics aims at providing universal descriptions of phase transitions on the basis of few and general parameters, the most important ones being dimensionality and symmetry[3–5]. The spontaneous symmetry breaking of Bose–Einstein condensates (BEC) below a critical temperature $T_C > 0$ is a remarkable example of such a transition, with the emergence of an extended coherence giving rise to a long-range order (LRO)[6–8]. Notably, in infinite systems with dimensionality $d \leq 2$, true LRO cannot be established at any finite temperature[9]. This is fundamentally due to the presence of low-energy, long-wavelength thermal fluctuations (that is, Goldstone modes) that prevail in $d \leq 2$ geometries.

## BKT phase transition

However, if we accept a lower degree of order, characterized by an algebraic decay of coherence, it is still possible to make a clear distinction between such a quasi-long-range-ordered (QLRO) and a disordered phase in which the coherence is lost in a much faster, exponential way. Such transitions, in two dimensions (2D) and at a critical temperature $T_{BKT} > 0$, are explained in the Berezinskii–Kosterlitz–Thouless theory (BKT) by the proliferation of vortices—the fundamental topological defects—of opposite signs[10]. This theory is well established for 2D ensembles of cold atoms in thermodynamic equilibrium, where the transition is linked to the appearance of a linear relationship between the energy and the wavevector of the excitations in the quasi-ordered state[11]. The joint observation of spatial and temporal decay of coherence has never been observed in atomic systems, mainly because of technical difficulties in measuring long-time correlations. These are important observables to bring together because an algebraic decay, with the same exponent $\alpha$, for both the temporal and spatial correlations of the condensed state, implies a linear dispersion for the elementary excitations[12–14].

## Phase transition in open systems

On the other hand, semiconductor systems such as microcavity polaritons (dressed photons with sizeable interactions mediated by the excitonic component) appear to be, since the report of their condensation[15–17], ideal platforms to extend the investigation of many-body physics to the more general scenario of phase transitions in driven–dissipative systems[18]. However, establishing if the transition can actually be governed by the same BKT process as for equilibrium system has proven to be challenging from both the theoretical[19–21] and experimental perspective[22–24]. Indeed, the dynamics of phase fluctuations is strongly modified by pumping and dissipation, and the direct measurement of their dispersion by photoluminescence and four-wave-mixing experiments is limited by the short polariton lifetime, by the pumping-induced noise, and by the low resolution close to the energy of the condensate. Moreover, the algebraic decay of coherence has been experimentally demonstrated only in spatial correlations, whereas only exponential or Gaussian decays of temporal coherence, which are not compatible with a BKT transition, have been reported until now[25–28]. The lack of a power-law decay of temporal correlations is a robust argument against a true BKT transition, as will be demonstrated later on with a straightforward counter-example of a strongly out-of-equilibrium system. For this reason, it has been a constant matter of interest what is the nature of the various polariton phases, what are the

[1]CNR NANOTEC—Institute of Nanotechnology, Via Monteroni, 73100 Lecce, Italy. [2]University of Salento, Via Arnesano, 73100 Lecce, Italy. [3]Department of Physics and Astronomy, University College London, Gower Street, London WC1E 6BT, UK. [4]Department of Physics, University of Warwick, Coventry CV4 7AL, UK. [5]CEMS, RIKEN, Saitama, 351-0198, Japan. [6]PRISM, Princeton Institute for the Science and Technology of Materials, Princeton University, Princeton, New Jersey 08540, USA. [7]Faculty of Science and Engineering, University of Wolverhampton, Wulfruna Street, WV1 1LY, UK. [8]Russian Quantum Center, Novaya 100, 143025 Skolkovo, Moscow Region, Russia. [9]INFN sezione di Lecce, 73100 Lecce, Italy. *e-mail: dario.ballarini@nanotec.cnr.it

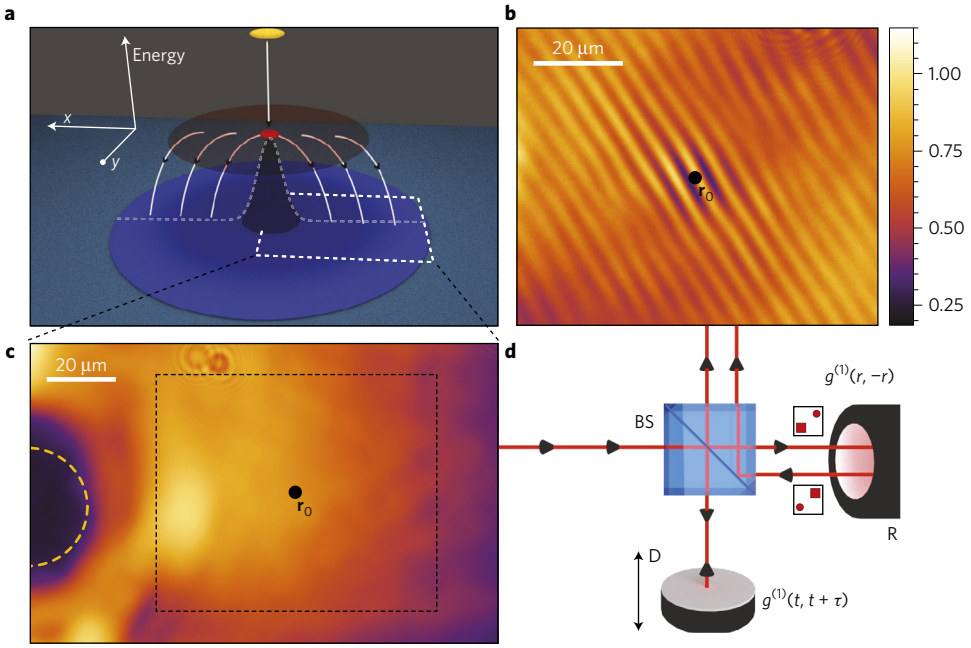


**Figure 1 | Pumping mechanism and interferometric set-up. a**, Sketch of polariton relaxation in space $(x, y)$ and energy (vertical axis). The carriers, injected by the pumping laser, relax quickly into excitonic states (yellow area) spatially confined within the pumping spot region. Efficient scattering from the exciton reservoir into polariton states results in a region of high polariton density (red area) which expands radially. During the expansion, the long lifetime allows for polariton relaxation into lower energy states and eventually, at high power, into the ground state. Above a threshold power, an extended 2D polariton condensate (blue area) is formed outside of the pumped region. **b**, Interferogram of the region in the black-dashed rectangle in **c**. The black dot at the centre indicates the autocorrelation point $\mathbf{r}_0$. **c**, 2D real-space image of the emitted light (arbitrary intensity units in a colour scale) from a portion of the condensate. To visualize only the bottom energy state in 2D images, the emission coming from $|k| < 1\,\mu m^{-1}$ has been selected in the far field to avoid the contribution of higher-energy polaritons. The yellow, dashed circle indicates the blue-shifted region corresponding to the position of the laser spot. **d**, Scheme of the interferometric set-up: R, retroreflector; BS, beam splitter; D, long delay line. The retroreflector R is a three-mirror corner reflector used to reflect the image at the central point $\mathbf{r}_0$ before sending it back towards the BS.

observables that allow one to determine a QLRO, if any, and how they compare with equilibrium 2D condensates and with lasers[29–35].

## Equilibrium vs out-of-equilibrium

Recently, thanks to a new generation of samples with record polariton lifetimes, the thermalization across the condensation threshold has been reported via constrained fitting to a Bose–Einstein distribution, suggesting a weaker effect of dissipation in these systems[36]. However, to unravel the mechanisms that drive the transition, and characterize its departure from the equilibrium condition, it is crucial to measure the correlations between distant points in space and time as we move from the disordered to the quasi-ordered regime[13,14,37,38]. So far, all attempts in this direction have been thwarted, not only because of the polariton lifetime being much shorter than the thermalization time and the fragmentation induced by sample inhomogeneities[39,40], but also because of the small extent of the condensate. Indeed, earlier measurements of coherence[25,41,42] were limited to the small spatial extension of the exciton reservoir set by the excitation spot, which could result in an effective trapping mechanism[43] and finite-size effects[30].

## BKT transition in exciton-polaritons

In this work, using a high-quality sample (in terms of long lifetimes and spatial homogeneity) to form and control a reservoir-free condensate of polaritons over a largely extended spatial region, we make the first observation in any system of the transition to a QLRO phase in both the spatial and temporal domains. Remarkably, the convergence of spatial and temporal decay of coherence allows us to identify the connection with the classic equilibrium BKT scenario, in which for systems with linear spectrum the exponents take exactly the same value $\alpha \leq 1/4$ (ref. 14). Stochastic simulations tuned to

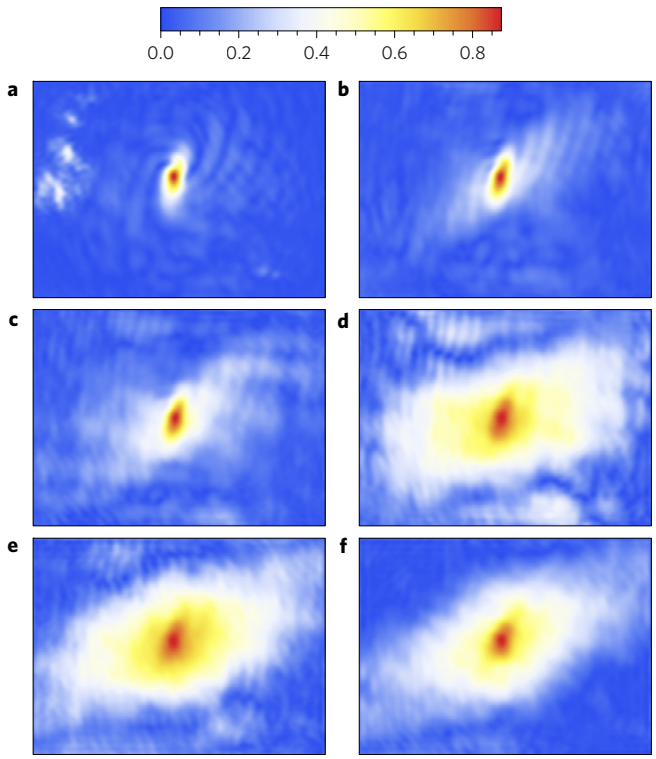


**Figure 2 | Two-dimensional first-order spatial correlations. a–f**, Maps of $|g^{(1)}(\mathbf{r})|$ as extracted from the interferogram (Fig. 1b) relative to an area of the sample of approximately 80 µm × 60 µm and corresponding to different densities $d = (0.05, 0.3, 0.5, 1.3, 3.0, 4.0)d_{th}$ in **a–f**, respectively.

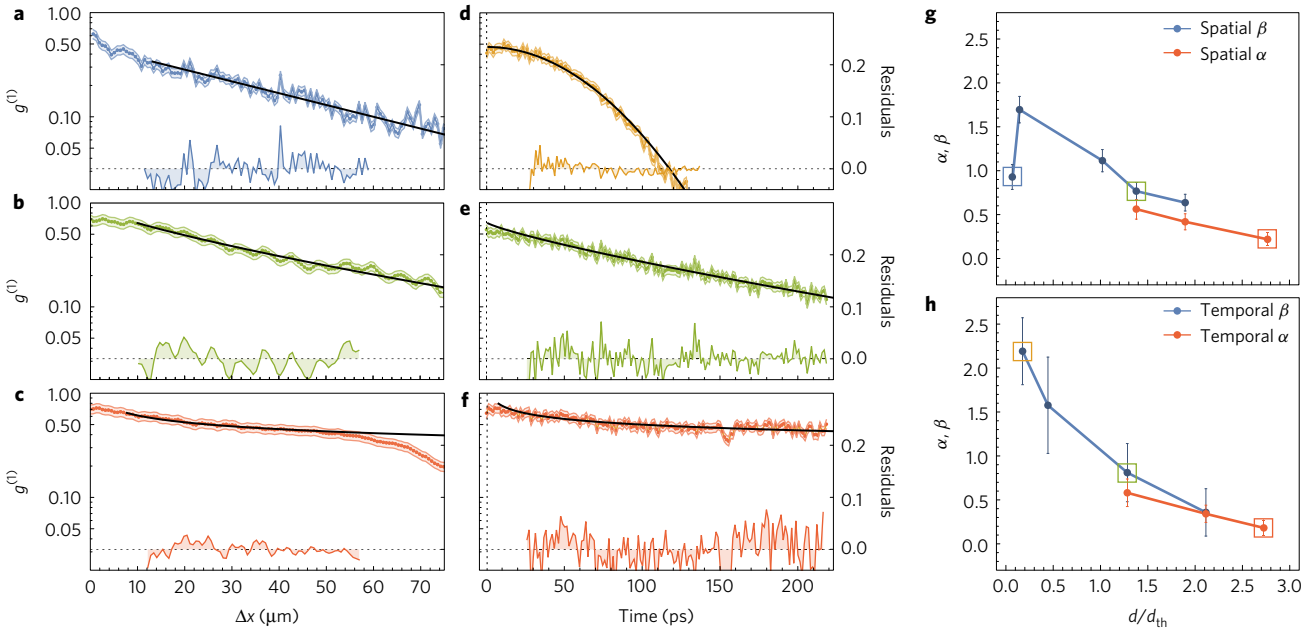


**Figure 3 | Coherence decay and BKT phase transition. a–c**, Spatial decay of $|g^{(1)}(\Delta x)|$ (logarithmic scale) and corresponding fitting residuals (linear scale) for: $d = 0.1d_{th}$ exponential decay (blue data) (**a**), $d = 1.4d_{th}$ stretched-exponential decay (green data) (**b**) and $d = 2.75d_{th}$ power-law decay (red data) (**c**). **d–f**, Temporal decay of $|g^{(1)}(\Delta t)|$ (logarithmic scale) and corresponding fitting residuals (linear scale) for: $d = 0.15d_{th}$ Gaussian decay (yellow data) (**d**), $d = 1.3d_{th}$ stretched-exponential decay (green data) (**e**) and $d = 2.7d_{th}$ power-law decay (red data) (**f**). Note that the value of $|g^{(1)}(0)| < 1$ is due to the time-averaged detection that globally reduces the visibility of the interferograms, without changing the slope of the correlations decay (see Supplementary Information). **g**,**h**, Blue line: $\beta$ exponent evaluated by stretched-exponential fitting of $|g^{(1)}(\Delta x)|$ in **g**, and $|g^{(1)}(\Delta t)|$ in **h**, versus the corresponding polariton densities. Red line: $\alpha$ exponent evaluated by power-law fitting of $|g^{(1)}(\Delta x)|$ in **g**, and $|g^{(1)}(\Delta t)|$ in **h**, versus the corresponding polariton densities. The same colour legend used in **a–f** indicates the corresponding densities (square markers) in **g** and **h**. Error bars are obtained from the fitting parameters (see Supplementary Information).

the experimental conditions, which reproduce the observations in both space and time, further allow us to track vortices in each realization of the condensate, confirming the topological origin of the transition. All these results settle the BKT nature of the 2D phase transition for polaritons in high-quality samples, providing the equilibrium limit of driven–dissipative systems. For shorter lifetimes, it is known that the transition departs from the equilibrium condition[28] and, at larger densities, different mechanisms will prevail over topological ordering[44]. We show here that for a strongly out-of-equilibrium microcavity (in the weak coupling regime), the power-law decay of the first-order coherence is observed only in space but not in time. We therefore demonstrate not only that low-density polariton condensates can undergo an equilibrium BKT transition like cold atoms, but also that spatial correlations alone do not allow one to distinguish between a photon laser and a BKT phase.

## Formation of a polariton condensate

The mechanism used to form an extended polariton condensate is sketched in Fig. 1a. The sample is excited non-resonantly (details in Supplementary Information), leading to the formation of an exciton reservoir (yellow region in Fig. 1a) which is localized within the pumping spot area due to the low exciton mobility. In turn, the repulsive interactions between excitons induce a blueshift of the polariton energy at the centre of the pumping spot (the dashed-white line in Fig. 1a shows the contour along the $x$ direction and crossing the excitation spot). As can be seen, the exciting beam generates an energy blueshift corresponding to the Gaussian profile of the laser. Polaritons, which are formed in the exciton reservoir through energy relaxation, are much lighter particles than excitons and are accelerated outwards from the centre of the spot by the potential landscape[45,46]. We have recently demonstrated that in high-quality 2D samples, the cloud of expanding polaritons relaxes through incoherent scattering processes into the ground state: when the stimulated scattering prevails over losses, a uniform polariton condensate is formed over a wide spatial region outside the area of the pumping spot[47]. The light emitted by the sample carries all the information about the spatio-temporal correlations of the polariton field, which can be extracted as follows: the interferograms (Fig. 1b) are obtained by selecting a sample region without the exciton reservoir, such as the one indicated by a dashed rectangle in Fig. 1c, that is directed into the Michelson interferometer outlined in Fig. 1d. Here, the image is duplicated in the beam splitter and reflected around the central point $\mathbf{r}_0$ in one arm of the interferometer, giving the interferogram shown in Fig. 1b. The first-order correlation function at equal time $g^{(1)}(\mathbf{r}, -\mathbf{r})$ ($\mathbf{r}_0 = 0$ is assumed) can then be measured between any two points symmetric about $\mathbf{r}_0$ as a function of their separation $|2\mathbf{r}|$ following the same method used in ref. 16 and reported in the Supplementary Information. The temporal coherence $g^{(1)}(t, t + \Delta t)$ is measured by moving the long delay line, covering a distance corresponding to a temporal delay of more than 200 ps.

## Spatial correlations and decay exponents

The 2D maps of $|g^{(1)}(\mathbf{r}, -\mathbf{r})|$, extracted from the interferograms, are shown in Fig. 2 for different values of the polariton density $d$ in the lowest-energy state. The spatial extent of coherence, limited to the autocorrelation point at low densities (Fig. 2a–c), extends over larger distances above a threshold density $d_{th}$ (Fig. 2d), indicating that stimulated scattering starts prevailing over losses (see Supplementary Information). For larger densities, a higher level of coherence is sustained over a wider spatial region of about 80 μm × 60 μm (Fig. 2e). The longer coherence length for $d > d_{th}$ is unrelated to the dynamics of higher-energy polaritons and corresponds to the formation of a uniform phase in the ground state over distances much larger than the healing length (see Supplementary Information). As shown in Fig. 2f, increasing further

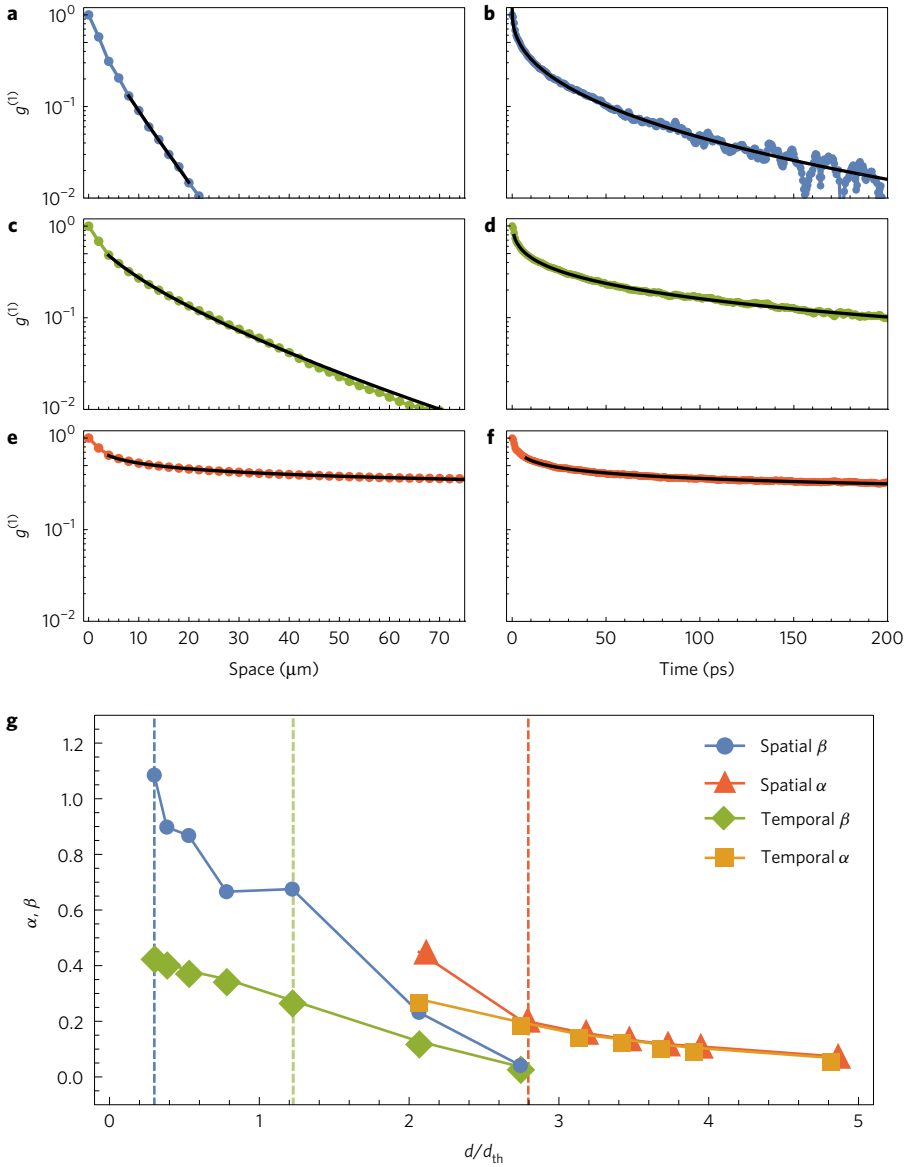


**Figure 4 | Decay of coherence from stochastic analysis of a homogeneous system. a**,**c**,**e**, Spatial decay of coherence. Respectively, an exponential decay, a stretched exponential with $\beta = 0.67$, and a power-law decay with $\alpha = 0.20$. **b**,**d**,**f**, Temporal decay of coherence. Respectively, a stretched exponential with $\beta = 0.41$, a stretched exponential with $\beta = 0.27$, and a power law with $\alpha = 0.20$. These three cases are indicated in **g** with blue, green and red vertical dashed lines. **g**, Exponents $\beta$ of the stretched-exponential fit, for spatial (blue) and temporal decay (green). Exponents $\alpha$ of the power-law fitting for spatial (red) and temporal decay (orange).

the excitation power results in the shrinking of the spatial extension of coherence due to the additional dephasing induced by the pump and the formation of excited states at higher energies[46].

In Fig. 3, we analyse the behaviour of coherence close to the density threshold in a more quantitative way. The horizontal line profile of $|g^{(1)}(x,-x)|$ passing through $\mathbf{r}_0$, for $\Delta x > 0$ (with $\Delta x \equiv 2x$), is studied for increasing pumping powers (Fig. 3a–c). To allow a uniform description across the transition, both power-law and stretched-exponential functions are used in the fitting procedure:

$$|g^{(1)}(x,-x)| = A|2x|^{-\alpha} \quad (1)$$

$$|g^{(1)}(x,-x)| = A\mathrm{e}^{-B|2x|^{\beta}} \quad (2)$$

with $B$ a scale parameter for the $x$-axis and $A \leq 1$ a space-independent amplitude factor (see Supplementary Information). For $d < d_{th}$, the decay is exponential and is well fitted by equation (2) with $\beta \approx 1$ (Fig. 3a). Approaching $d = d_{th}$, the spatial decay of $g^{(1)}$ becomes slower, but still faster than a power law (Fig. 3b). This transition regime is best described by a stretched-exponential decay ($\beta < 1$) that becomes a power law only at slightly higher densities $d \approx 2.7 d_{th}$ (Fig. 3c) when a high degree of spatial coherence (>50%) extends over distances of approximately 50 μm. Remarkably, the slow decay shown in Fig. 3c can be best characterized by the exponent $\alpha = 0.22$ (see Supplementary Information for a comparison between the different functional behaviours). In Fig. 3g, the $\alpha$ and $\beta$ exponents are reported for different densities ($\alpha$ can be extracted only for $d > d_{th}$), showing the whole behaviour of the coherence decay across the transition into the QLRO. However, as will be shown in the following, it is essential to verify that a similar behaviour is also observed for the temporal correlations.

## Temporal correlations

In Fig. 3d–f, the temporal coherence at the autocorrelation point $|g^{(1)}(t, t+\Delta t)|$ is shown for three different polariton densities. In

Fig. 3h, the $\alpha$ and $\beta$ exponents of equations (1) and (2) that best fit the experimental data are shown across the transition. Below threshold, coherence decays quickly and follows a Gaussian slope ($\beta \approx 2$). At $d = 1.3d_{\mathrm{th}}$, the temporal coherence can be best fitted by equation (2) with an exponent $\beta \approx 0.8$ (or, with a slightly worst fit, with a power law of exponent $\alpha \approx 0.57$), whereas at $d \approx 2.7d_{\mathrm{th}}$, the long-time behaviour clearly follows a power law with $\alpha = 0.2$. The residuals analysis proves the agreement between the experimental data and the fitting model (see Supplementary Information). Crucially, also for time correlations, $\alpha < 0.25$, which coincides, within the experimental accuracy, with the one obtained from the spatial coherence at the corresponding density.

## Theoretical analysis

We performed complementary theoretical analysis, based on the exact solution of the stochastic equations of motion[21], with the same microscopic parameters as the ones of the experiment. Our approach, which can be derived either from Keldysh field theory[48] or the Fokker–Planck equations for the Wigner function[18], is able to treat fluctuations beyond the mean field approximations and describes the dynamics of the whole field, accounting for both normal and superfluid polaritons (see Supplementary Information). Differently from previous works[25], the condensate forms outside of the exciton reservoir—which is therefore not included in the model. Moreover, the process of injection and expansion of polaritons is described as an effective pumping mechanism, without assuming any particular constraint on the incoherent polariton population, and also the energy relaxation is not externally imposed by any specific term, given that the whole physics, including thermalization and condensation, can be self-consistently obtained from the stochastic model (see Supplementary Information). This is indeed the most general setting used in statistical mechanics to describe the effect of external driving, dissipation and many-body interactions on the phase transitions in open quantum systems[38,48]. Here we observe the same crossover from an exponential via stretched exponential to an algebraic decay of coherence in space and time (Fig. 4) as for the experimental measurements. In particular, we see the spatial and temporal $\alpha$ being the same, and always smaller than 1/4 above the BKT threshold (Fig. 4g), showing that drive and dissipation do not prevail in this good-quality sample, in contrast to the earlier studied non-equilibrium cases[21,25].

Additionally, although the vortex–antivortex binding cannot be directly observed in the experiments, which average over many realizations, the numerical analysis is able to track the presence of free vortices in each single realization, confirming the topological origin of the transition. Indeed, we see clearly that, in the algebraically ordered state, free vortices do not survive and the pairing is complete (Fig. 5 right column). In contrast, the exponential and stretched-exponential regimes both show the presence of free vortices (Fig. 5 left), the number of which decreases as we move across the transition. Since the stretched-exponential phase is always associated with some presence of free vortices, this supports that we are observing a BKT crossover rather than a Kardar–Parisi–Zhang (KPZ) phase[19]. It is interesting to note here that the KPZ physics is indeed the paradigmatic model for a genuinely non-equilibrium phase transition, and its manifestation in the optical domain of polariton condensates is currently at the centre of intense investigation[38]. However, the expected critical length for the KPZ phase is beyond the experimentally achievable length scales in our long-lifetime, incoherently driven microcavity (see Supplementary Information for further discussion).

## Spatial and temporal correlations in a laser

Finally, to demonstrate the importance of the simultaneous observation of space and time correlations for optical systems, and in general as we move from equilibrium towards out-of-equilibrium, we analyse the coherence behaviour of a microcavity where driven–dissipative dynamics clearly prevail. Using a sample with a lower quality factor and less quantum wells, we induce, under high non-resonant pumping, the photon-laser regime as in a vertical cavity surface emitting laser (VCSEL)[44,49]. Despite the fact that this system is strongly out-of-equilibrium, it shows a power-law decay of spatial coherence with $\alpha = 0.25$ (Fig. 6a), although limited by the pumping spot region (with a radius of about 10 μm). Remarkably, the behaviour of spatial correlations is very similar to what was obtained in ref. 25, but the temporal coherence, shown in Fig. 6b, follows a quasi-Gaussian decay, not compatible with the algebraic order characteristic of the BKT phase. This shows that a consistent behaviour between time and space is necessary to evidence the BKT transition in driven–dissipative systems.

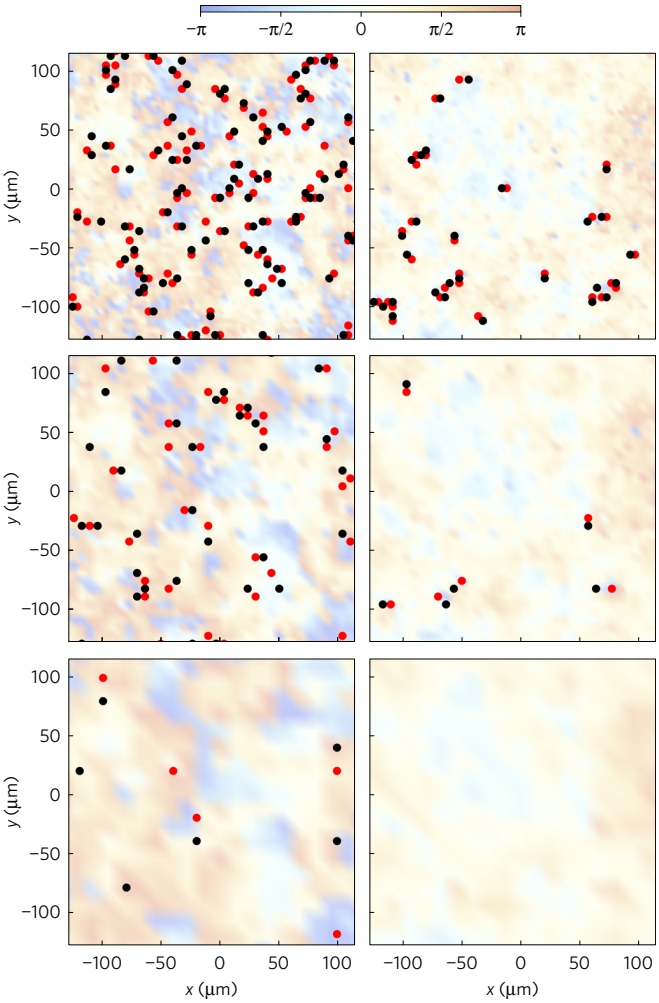


**Figure 5 | Vortex–antivortex distribution map.** Top: vortices (V) in red and anti-vortices (AV) in black just before (left) and after (right) the BKT transition with parameters as in Fig. 4c,e, respectively. Middle to bottom: the same as top but after filtering off, in two steps, high-momentum states to eliminate bound pairs. Such filtering reveals the presence of free vortices. Note that there are no free vortices when spatial and temporal coherence show algebraic decay (right), but there are some free vortices in the case of stretched-exponential decay of coherence (left). The underlying colour map shows the phase profile of the field.

## Conclusions and outlook

The formation of an ordered phase in 2D driven–dissipative ensembles of bosonic quasiparticles is observed in both spatial and temporal correlations across the transition. The collective

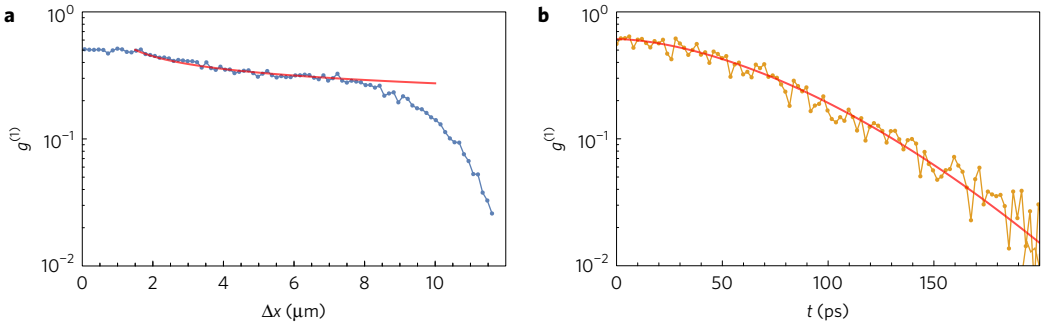


**Figure 6 | Spatial and temporal coherence in weak coupling regime. a**, Spatial coherence showing a power-law decay with $\alpha = 0.25$. **b**, Temporal decay of coherence with stretched-exponential fitting exponent $\beta = 1.8$.

behaviour of exciton-polaritons in semiconductor microcavities lies at the interface between equilibrium and out-of-equilibrium phase transitions, and it has been often compared both to atomic condensates and to photon lasers. We show that the measurement of spatial correlations $g^{(1)}(\mathbf{r})$ alone is not sufficient to establish whether an open/dissipative system is in the BKT phase. Instead, two distinct measurements, one in time and one in the space domain, are needed. Satisfying this requirement, we report a power-law decay of coherence with the onset of the algebraic order at the same relative density and comparable exponents for both space and time correlations. We should stress that the exceptionally long polariton lifetime in the present sample allows us to reach the BKT phase transition at low densities, and in a region without the excitonic reservoir, resulting in a lower level of dephasing and longer time for thermalization. Moreover, in our experiments, the absence of any trapping mechanism, be it from the exciton reservoir or potential minima, allows us to avoid the influence of finite-size effects in the temporal dynamics of the autocorrelation[14]. Simulations with stochastic equations match perfectly the experimental results and demonstrate that the underlying mechanism of the transition is of the BKT type—that is, a topological ordering of free vortices into bound pairs, resulting in the coherence build up both in space and time. All these observations validate that polaritons can undergo phase transitions following the standard BKT picture, and fulfil the expected conditions of thermal equilibrium despite their driven–dissipative nature. Now that the equilibrium character of polaritons becomes a tuneable parameter, the study of driven–dissipative equilibrium phase transitions and of the universal scaling laws is within reach in this solid state device.

**Data availability.** The raw experimental and numerical data used in this study are available from the corresponding author upon reasonable request.

Received 30 November 2016; accepted 24 October 2017; published online 4 December 2017

## References


1. Stanley, H. E. Scaling, universality, and renormalization: three pillars of modern critical phenomena. *Rev. Mod. Phys.* **71,** S358–S366 (1999).
2. Castellano, C., Fortunato, S. & Loreto, V. Statistical physics of social dynamics. *Rev. Mod. Phys.* **81,** 591–646 (2009).
3. Onsager, L. Crystal statistics. I. A two-dimensional model with an order–disorder transition. *Phys. Rev.* **65,** 117–149 (1944).
4. Landau, L. D. & Lifshitz, E. M. *Statistical Physics* Vol. 5 (Butterworth-Heinemann, 1980).
5. Hohenberg, P. & Halperin, B. Theory of dynamic critical phenomena. *Rev. Mod. Phys.* **49,** 435–479 (1977).
6. Pitaevskii, L. & Stringari, S. *Bose–Einstein Condensation and Superfluidity* (Oxford Univ. Press, 2016).
7. Kohl, M. *et al*. Criticality and Correlations in Cold Atomic Gases. in *Advances in Solid State Physics* Vol. 47 (ed. Haug, R.) 79–88 (Springer, 2008); https://link.springer.com/chapter/10.1007/978-3-540-74325-5_7
8. Braun, S. *et al*. Emergence of coherence and the dynamics of quantum phase transitions. *Proc. Natl Acad. Sci. USA* **112,** 3641–3646 (2015).
9. Mermin, N. D. & Wagner, H. Absence of ferromagnetism or antiferromagnetism in one- or two-dimensional isotropic heisenberg models. *Phys. Rev. Lett.* **17,** 1133–1136 (1966).
10. Minnhagen, P. The two-dimensional coulomb gas, vortex unbinding, and superfluid-superconducting films. *Rev. Mod. Phys.* **59,** 1001–1066 (1987).
11. Steinhauer, J., Ozeri, R., Katz, N. & Davidson, N. Excitation spectrum of a Bose–Einstein condensate. *Phys. Rev. Lett.* **88,** 120407 (2002).
12. Nelson, D. R. & Kosterlitz, J. M. Universal jump in the superfluid density of two-dimensional superfluids. *Phys. Rev. Lett.* **39,** 1201–1205 (1977).
13. Szymanska, M. H., Keeling, J. & Littlewood, P. B. Nonequilibrium quantum condensation in an incoherently pumped dissipative system. *Phys. Rev. Lett.* **96,** 230602 (2006).
14. Szymańska, M. H., Keeling, J. & Littlewood, P. B. Mean-field theory and fluctuation spectrum of a pumped decaying Bose–Fermi system across the quantum condensation transition. *Phys. Rev. B* **75,** 195331 (2007).
15. Richard, M., Kasprzak, J., Romestain, R., Andre, R. & Dang, L. S. Spontaneous coherent phase transition of polaritons in CdTe microcavities. *Phys. Rev. Lett.* **94,** 187401 (2005).
16. Kasprzak, J. *et al*. Bose–Einstein condensation of exciton polaritons. *Nature* **443,** 409–414 (2006).
17. Balili, R., Hartwell, V., Snoke, D., Pfeiffer, L. & West, K. Bose–Einstein condensation of microcavity polaritons in a trap. *Science* **316,** 1007–1010 (2007).
18. Carusotto, I. & Ciuti, C. Quantum fluids of light. *Rev. Mod. Phys.* **85,** 299–366 (2013).
19. Altman, E., Sieberer, L. M., Chen, L., Diehl, S. & Toner, J. Two-dimensional superfluidity of exciton polaritons requires strong anisotropy. *Phys. Rev. X* **5,** 011017 (2015).
20. Wachtel, G., Sieberer, L., Diehl, S. & Altman, E. Electrodynamic duality and vortex unbinding in driven–dissipative condensates. *Phys. Rev. B* **94,** 104520 (2016).
21. Dagvadorj, G. *et al*. Nonequilibrium phase transition in a two-dimensional driven open quantum system. *Phys. Rev. X* **5,** 041028 (2015).
22. Utsunomiya, S. *et al*. Observation of Bogoliubov excitations in exciton-polariton condensates. *Nat. Phys.* **4,** 700–705 (2008).
23. Kohnle, V. *et al*. From single particle to superfluid excitations in a dissipative polariton gas. *Phys. Rev. Lett.* **106,** 255302 (2011).
24. Kohnle, V. *et al*. Four-wave mixing excitations in a dissipative polariton quantum fluid. *Phys. Rev. B* **86,** 064508 (2012).
25. Roumpos, G. *et al*. Power-law decay of the spatial correlation function in exciton-polariton condensates. *Proc. Natl Acad. Sci. USA* **109,** 6467–6472 (2012).
26. Krizhanovskii, D. N. *et al*. Dominant effect of polariton-polariton interactions on the coherence of the microcavity optical parametric oscillator. *Phys. Rev. Lett.* **97,** 097402 (2006).
27. Love, A. P. D. *et al*. Intrinsic decoherence mechanisms in the microcavity polariton condensate. *Phys. Rev. Lett.* **101,** 067404 (2008).
28. Kim, S. *et al*. Coherent polariton laser. *Phys. Rev. X* **6,** 011026 (2016).
29. Dihel, S. *et al*. Quantum states and phases in driven open quantum systems with cold atoms. *Nat. Phys.* **4,** 878–883 (2008).
30. Keeling, J., Szymańska, M. H. & Littlewood, P. B. *Keldysh Green's Function Approach to Coherence in a Non-Equilibrium Steady State: Connecting Bose–Einstein Condensation and Lasing* 293–329 (Springer, 2010).
31. Kirton, P. & Keeling, J. Nonequilibrium model of photon condensation. *Phys. Rev. Lett.* **111,** 100404 (2013).
32. Deng, H., Weihs, G., Snoke, D., Bloch, J. & Yamamoto, Y. Polariton lasing vs. photon lasing in a semiconductor microcavity. *Proc. Natl Acad. Sci. USA* **100,** 15318–15323 (2003).

33. Butov, L. V. Solid-state physics: a polariton laser. *Nature* **447,** 540–541 (2007).
34. Klaers, J., Schmitt, J., Vewinger, F. & Weitz, M. Bose–Einstein condensation of photons in an optical microcavity. *Nature* **468,** 545–548 (2010).
35. Fraser, M. D., Hofling, S. & Yamamoto, Y. Physics and applications of exciton-polariton lasers. *Nat. Mater.* **15,** 1049–1052 (2016).
36. Sun, Y. *et al*. Bose–Einstein condensation of long-lifetime polaritons in thermal equilibrium. *Phys. Rev. Lett.* **118,** 016602 (2017).
37. Chiocchetta, A. & Carusotto, I. Non-equilibrium quasi-condensates in reduced dimensions. *Europhys. Lett.* **102,** 67007 (2013).
38. Keeling, J. *et al*. in *Superfluidity and Phase Correlations of Driven Dissipative Condensates* (eds Proukakis, N.P., Snoke, D. W. & LIttlewood, P. B.) (Cambridge Univ. Press, 2017).
39. Krizhanovskii, D. N. *et al*. Coexisting nonequilibrium condensates with long-range spatial coherence in semiconductor microcavities. *Phys. Rev. B* **80,** 045317 (2009).
40. Sanvitto, D. *et al*. Spatial structure and stability of the macroscopically occupied polariton state in the microcavity optical parametric oscillator. *Phys. Rev. B* **73,** 241308(R) (2006).
41. Deng, H., Solomon, G. S., Hey, R., Ploog, K. H. & Yamamoto, Y. Spatial coherence of a polariton condensate. *Phys. Rev. Lett.* **99,** 126403 (2007).
42. Nitsche, W. H. *et al*. Algebraic order and the Berezinskii–Kosterlitz–Thouless transition in an exciton-polariton gas. *Phys. Rev. B* **90,** 205430 (2014).
43. Hadzibabic, Z. *et al*. Berezinskii–Kosterlitz–Thouless crossover in a trapped atomic gas. *Nature* **441,** 1118–1121 (2006).
44. Bajoni, D. *et al*. Polariton light-emitting diode in a GaAs-based microcavity. *Phys. Rev. B* **77,** 113303 (2008).
45. Tosi, G. *et al*. Sculpting oscillators with light within a nonlinear quantum fluid. *Nat. Phys.* **8,** 190–194 (2012).
46. Wertz, E. *et al*. Spontaneous formation and optical manipulation of extended polariton condensates. *Nat. Phys.* **6,** 860–864 (2010).
47. Ballarini, D. *et al*. Formation of a macroscopically extended polariton condensate without an exciton reservoir. *Phys. Rev. Lett.* **118,** 215301 (2017).
48. Sieberer, L. M., Buchhold, M. & Diehl, S. Keldysh field theory for driven open quantum systems. *Rep. Prog. Phys.* **79,** 096001 (2016).
49. Butté, R. *et al*. Transition from strong to weak coupling and the onset of lasing in semiconductor microcavities. *Phys. Rev. B* **65,** 205310 (2002).


## Acknowledgements

This work has been funded by the MIUR project Beyond Nano and the ERC project POLAFLOW (Grant N. 308136). M.H.S. acknowledges support from EPSRC (Grants No. EP/I028900/2 and No. EP/K003623/2).

## Author contributions

D.C. and D.B. took and analysed the data. G.D. and M.H.S. performed stochastical numerical simulations. C.S.M. and F.P.L. discussed the results. D.C., D.B., C.S.M., M.D.G., L.D., G.G., F.P.L., M.H.S. and D.S. co-wrote the manuscript. K.W. and L.N.P. fabricated the sample. D.S. coordinated and supervised all the work.

## Additional information

Supplementary information is available in the online version of the paper. Reprints and permissions information is available online at www.nature.com/reprints. Publisher's note: Springer Nature remains neutral with regard to jurisdictional claims in published maps and institutional affiliations. Correspondence and requests for materials should be addressed to D.B.

## Competing financial interests

The authors declare no competing financial interests.